Acta Chemica Scandinavica A 39 (1985) 389–395

Crystal and Magnetic Structure of $MnSb_2O_4$

HELMER FJELLVÅG[a] and ARNE KJEKSHUS[b]

[a] Institutt for Energiteknikk, N-2007 Kjeller, Norway and [b] Kjemisk Institutt, Universitetet i Oslo, Blindern, N-0315 Oslo 3, Norway

$MnSb_2O_4$ takes the $ZnSb_2O_4$ type structure below 985 K. Curie-Weiss law is satisfied between 80 and 985 K; μ_{eff}=6.02±0.10 μ_B, θ=−190±20 K. At temperatures below T_N=55±2 K the moments order antiferromagnetically and the arrangement can be described as superimposed $A_{x,y}$ and G_z modes, with magnetic moments of 4.37(6) and 1.15(25) μ_B, respectively, at 10 K.

A large number of well characterized phases in the ternary T–Sb–O systems (T=3d metal) adopt the rutile ($T$$SbO_4$, disordered), trirutile ($T$$Sb_2O_6$, ordered) and niobite ($T$$Sb_2O_6$, ordered) type structures. Although compounds with the composition $T$$Sb_2O_4$ have been known for decades,[1–4] they have, until recently,[5–8] been rather superficially explored. The present contribution concerns the structural and magnetic properties of $MnSb_2O_4$ in relation to the isostructural phases $FeSb_2O_4$,[8] $NiSb_2O_4$[7] and $ZnSb_2O_4$.[2] After the experimental part of this study was completed and the first manuscript draft was written, two papers[7,8] on $MnSb_2O_4$ have appeared. This has occasioned substantial rewriting of the manuscript, but the present results are believed to differ sufficiently from those in Refs. 7, 8 to justify a brief separate report.

EXPERIMENTAL

$T$$Sb_2O_4$ can be prepared according to a number of procedures, *e.g.*, heating of stoichiometric amounts of TO and Sb_2O_3 (or similarly T and Sb_2O_4) in evacuated, sealed silica tubes, or by reduction of more oxygen rich phases. In this study, $MnSb_2O_4$ was prepared by reaction between Mn (Johnson, Matthey & Co., crushed flakes, 99.99 %) and α-Sb_2O_4 [prepared by heating of Sb_2O_3 (Riedel de Haen AG, *p.a.*) in air at 950 °C for 2×2 d with intermediate crushings]. Al_2O_3 crucibles were placed inside the silica tubes in order to prevent reaction with, or recrystallization of, the silica. After annealing at 630 °C for 1 d, the samples were carefully ground and subjected to one further heat treatment at 630 °C for 2 d and finally slowly cooled to room temperature. The maximum temperature of 630 °C was chosen in order to avoid thermal decomposition into MnO and (cubic) Sb_2O_3. However, the large scale (~10 g) powder neutron diffraction sample was slightly contaminated with MnO and a few fairly large single crystals of Sb_2O_3.

Gavarri *et al.*[7,8] synthesized $MnSb_2O_4$ both from MnO and Sb_2O_3 (hydrothermally; 510 °C, 1 kbar) and by heating a mixture of Mn, Mn_3O_4 and Sb_2O_3 at 475 °C. The latter method, however, is reported to give a large residue of the reactants. [The preparational details should be registered carefully since the properties of $MnSb_2O_4$ appear (*cf.* Ref. 8) to depend on the sample quality.]

Powder X-ray diffraction photographs were obtained at room temperature in a Guinier camera (Cu$K\alpha_1$-radiation, λ=154.0598 pm, Si as internal standard a=543.1065 pm[9]). Low

0302-4377/85 $2.50

and high temperature X-ray diffraction photographs were taken with a Guinier Simon camera (Enraf-Nonius FR 553) between 100 and 1000 K.

Magnetic susceptibility data were recorded between 80 and ~1000 K using an ordinary Faraday balance (maximum field ~8 kOe).

Powder neutron diffraction data were collected with the OPUS III two-axis spectrometer accommodated at the JEEP II reactor, Kjeller. Monochromatic neutrons of wavelength 187.7 pm were obtained by reflection from (111) of a Ge-crystal. The scattered intensities were registered by a multi-counter system consisting of five ^{3}He-detectors spaced 10° apart in 2θ. The data were recorded in steps of 0.05° from 2θ=5.00 to 80.00°. Cylindrical sample holders of V were used. A Displex cooling unit was used to obtain temperatures between 10 and 293 K.

The structural analyses of the powder neutron diffraction data were performed according to the Hewat[10] version of the Rietveld[11] programme. Two unit cell dimensions, five positional parameters, four isotropic temperature factors, one scale factor and three half-width parameters entered as variables in the least squares refinements. The scattering lengths (in 10^{-12} cm) $b_{Mn}=-0.373$, $b_{Sb}=0.564$ and $b_O=0.5805$ were adopted,[12] as was the magnetic form factor for Mn^{2+}.[13] Appropriate regions of the diffraction pattern containing peaks from Al or MnO[14] were excluded from the profile refinements.

RESULTS

(i) *Crystal structure.* Unit cell dimensions and positional parameters for the $ZnSb_2O_4$ type structure (space group $P4_2/mbc$; *hhl* absent for $l=2n+1$ and $0kl$ absent for $k=2n+1$) of $MnSb_2O_4$ at 10, 60 and 293 K were derived by Rietveld analyses of powder neutron diffraction data, and are listed in Table 1, together with the corresponding data from Ref. 7. (Data for $NiSb_2O_4$, $FeSb_2O_4$ and $ZnSb_2O_4$ are found in Refs. 2, 4, 6, 7.) The shortest interatomic distances for $MnSb_2O_4$ are given in Table 2.

The atomic arrangement of the $ZnSb_2O_4$ type structure is depicted in Fig. 1, which also brings out the relationship to the Pb_3O_4 type[15] structure. The *T* and Sb atoms occupy, respectively, the octahedral and pyramidal Pb positions of the Pb_3O_4 type structure. The MnO_6 octahedra form, through the sharing of opposite edges, chains parallel to the tetragonal *c* axis. Within these chains the *T* atoms are separated by $c/2\approx300$ pm, while the distances between the *T* atoms of neighbouring chains are $a/\sqrt{2}\approx600$ pm.

The (presumably) three-valent Sb atoms are pyramidally co-ordinated to three O atoms [2×202.9(8) and 1×186.6(19) pm for $MnSb_2O_4$ at 10 K], thus resembling the Sb

Table 1. Unit cell dimensions and positional parameters with standard deviations for $MnSb_2O_4$ as derived by Rietveld analysis of powder neutron diffraction data. Space group $P4_2/mbc$, Mn in 4*d*, Sb in 8*h*, O_I in 8*h* and O_{II} in 8*g*. (Nuclear R_n-factors ranging between 0.04 and 0.08, magnetic R_m-factors ranging between 0.06 and 0.10. 30–35 nuclear and 6–8 magnetic reflections. Debye-Waller factors (in 10^4 pm^2): 0.2 at 10 K, 0.6–1.0 at 293 K.)

T (K)	10	60	293	5 (Ref. 7)
a (pm)	870.23(7)	870.13(6)	870.97(8)	869.70
c (pm)	598.31(6)	598.63(6)	599.82(9)	598.10
x_{Sb}	0.191(2)	0.189(1)	0.194(2)	0.168(2)
y_{Sb}	0.166(1)	0.169(1)	0.165(2)	0.160(2)
x_{O_I}	0.096(1)	0.100(1)	0.100(2)	0.088(2)
y_{O_I}	0.641(1)	0.642(1)	0.639(2)	0.649(2)
$x_{O_{II}}$	0.677(1)	0.678(1)	0.679(2)	0.680(2)

Table 2. Interatomic distances (<350 pm) for $MnSb_2O_4$ at 10 K. Calculated standard deviations in the last (or the two last) digit(s) in parentheses.

$Mn-O_I \times 4$	210.7(11)	$O_I-O_I \times 2$	282.5(11)
$Mn-O_{II} \times 2$	217.8(9)	$O_I-O_{II} \times 2$	294.1(13)
$Mn-Mn \times 2$	299.15(3)	$O_I-O_I \times 1$	296.9(30)
$Mn-Sb \times 4$	399.9(14)	$O_I-Sb \times 1$	301.0(19)
		$O_I-O_I \times 2$	304.2(5)
$Sb-O_I \times 1$	186.6(19)	$O_I-O_{II} \times 2$	322.4(17)
$Sb-O_{II} \times 2$	202.9(8)	$O_I-Sb \times 2$	338.5(11)
$Sb-O_I \times 1$	301.0(19)		
$Sb-O_I \times 2$	338.5(11)	$O_{II}-Sb \times 2$	202.9(8)
$Sb-Mn \times 2$	339.9(14)	$O_{II}-Mn \times 1$	217.8(9)
$Sb-Sb \times 2$	347.1(10)	$O_{II}-O_I \times 2$	282.5(11)
		$O_{II}-O_I \times 2$	294.1(13)
$O_I-Sb \times 1$	186.6(19)	$O_{II}-O_{II} \times 2$	299.2(1)
$O_I-Mn \times 2$	210.7(11)	$O_{II}-O_I \times 2$	322.4(17)

coordination (three Sb–O bonds and one "lone-pair") in orthorhombic (valentinite) and cubic (senarmonite) Sb_2O_3.[16,17] These findings are in line with the structural data for $FeSb_2O_4$,[4] $NiSb_2O_4$[6,7] and $ZnSb_2O_4$[2] (as well as for Pb_{II} in Pb_3O_4[15]), but differ appreciably from those in Refs. 7,8. The available data suggest that the *T* atoms in the deformed octahedral co-ordination (4+2 T–O distances) of the $ZnSb_2O_4$ type phases are in high spin *T* states. The variations in unit cell dimensions for the TSb_2O_4 phases mainly result from changes in the *T*–O bond lengths (positional parameters being little affected, except for *T*=Zn).

High temperature powder X-ray diffraction photographs show that $MnSb_2O_4$ (when sealed in silica tubes) is stable up to ~985 K, and this finding is confirmed by DTA data. At higher temperatures decomposition as well as reaction with the silica tubes take place. As seen from Fig. 2 the unit cell dimensions increase smoothly and monotonically between 10 and 985 K, and no sign of any crystallographic phase transition was recorded in this temperature interval. The thermal expansion properties of $MnSb_2O_4$ for the range 10–300 K (Fig. 2) differ from those reported by Gavarri *et al.*[7] The two studies are in reasonable agreement concerning the numerical values of the unit cell dimensions at 10 and 300 K, implying that the average thermal expansion coefficients for this range concur. The present

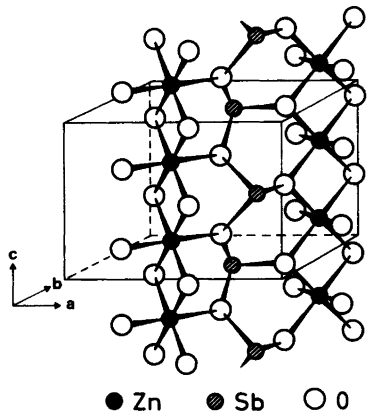

Fig. 1. Perspective view of the $ZnSb_2O_4$ type structure.

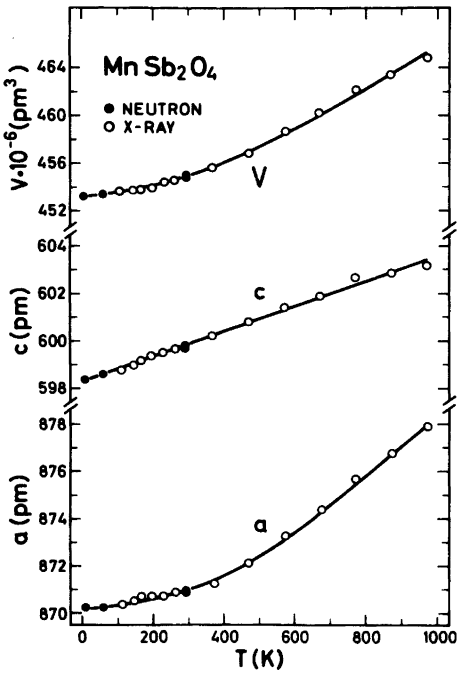

Fig. 2. Unit cell dimensions of $MnSb_2O_4$ *versus* temperature between 10 and 985 K. *Calculated* error limits do not exceed the size of symbol. (1 Å=100 pm.)

study demonstrates a very nearly linear thermal expansion of the *c* axis between 10 and 985 K [$\alpha_c=(1/c_{293})\cdot(\partial c/\partial T)\approx 9\times10^{-6}$ K^{-1}] while Gavarri *et al.*[7] found that α_c passes through a maximum at 70 K. [The anomalous thermal behaviour of *c* reported in Ref. 7 occurs between 5 and 115 K and is accordingly in any case only weakly correlated with the onset of co-operative magnetism in $MnSb_2O_4$; *cf.* (ii).] According to Fig. 2 *a* and *V* expand non-linearly up to ~600 K and then approximately linearly for $\sim600<T<\sim985$ K [$\alpha_a=(1/a_{293})\cdot(\partial a/\partial T)\approx 14\times10^{-6}$ K^{-1}, $\alpha_V=(1/V_{293})\cdot(\partial V/\partial T)\approx 2\alpha_a+\alpha_c\approx 38\times10^{-6}$ K^{-1}].

As seen from Table 1, $MnSb_2O_4$ retains the $ZnSb_2O_4$ type crystal structure between 293 and 10 K, and the positional parameters stay constant within two calculated standard deviations. For $FeSb_2O_4$, which is isostructural with $MnSb_2O_4$ at room temperature, a small orthorhombic distortion (~0.2 % difference between *a* and *b* at 4.2 K) is established at low temperatures.[4] The distortion of $FeSb_2O_4$ is not necessarily directly correlated with the paramagnetic to antiferromagnetic transition. Gavarri and Hewat[8] report that the degree of orthorhombic distortion for $MnSb_2O_4$ and $NiSb_2O_4$ depends on the sample quality (*e.g.* non-stoichiometry, impurities, *etc.*) and that it is evident even at room temperature. However, careful examination of the present $MnSb_2O_4$ samples gave no sign of any deviation from the tetragonal symmetry.

(ii) *Magnetic properties.* The magnetic susceptibility *versus* temperature relationship fulfils the Curie-Weiss law between 80 and 985 K with $\theta=-190\pm20$ K, $\mu_{eff}=6.02\pm0.10$ μ_B and $2S=3.10\pm0.10$ (assuming no orbital contribution). The paramagnetic moment agrees well with the value $\mu_{eff}=5.92$ μ_B, expected for high spin Mn^{2+} (ground state $^6S_{5/2}$). The impurities of MnO and Sb_2O_3 in the bulk sample were separated from $MnSb_2O_4$ by manipulation under a microscope prior to the magnetic susceptibility measurements.

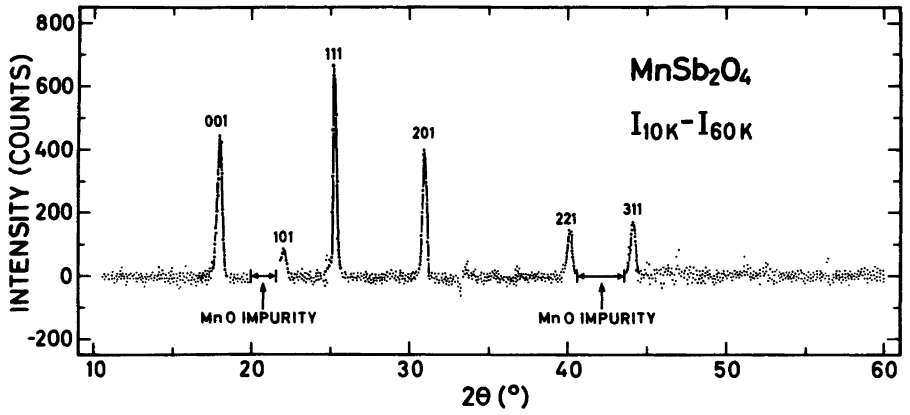

Fig. 3. Difference diagram between powder neutron diffraction patterns of $MnSb_2O_4$ at 10 and 60 K.

Additional reflections in the powder neutron diffraction diagram at 10 K immediately indicate antiferromagnetic long range order, as illustrated by the difference diagram (Fig. 3) between the data collected at 10 and 60 K. The additional reflections can all be indexed on the basis of the crystallographic unit cell, but the extinction rules of space group $P4_2/mbc$ are violated. The Néel temperature $T_N=55\pm2$ K is obtained from the temperature dependence of 001 (Fig. 4).

The representation analysis derived by Bertaut[18] predicts four different, possible moment configurations for the TSb_2O_4 compounds. With the numbering of Mn atoms as (1) $\frac{1}{2}0\frac{1}{4}$; (2) $\frac{1}{2}0\frac{3}{4}$; (3) $0\frac{1}{2}\frac{1}{4}$ and (4) $0\frac{1}{2}\frac{3}{4}$, the directions + or − for the moments of the Mn atoms in the unit cell can be combined as ++++ (*F*); ++−− (*C*); +−−+ (*G*) and +−+− (*A*). The difference pattern (Fig. 3) is in accordance with an *A* mode which favours *hkl* reflections with $h+k=2n$ and $l=2n+1$. The presence of 101 indicates the coexistence of a *G* mode. The directions and magnitudes of the magnetic moments at 10 K were derived through Rietveld analysis of the powder neutron diffraction data, yielding $A_{x,y}:\mu_{x,y}=4.37(6)\mu_B$ and $G_z:\mu_z=1.15(25)\ \mu_B$; *calculated* standard deviations in parentheses. The powder neutron

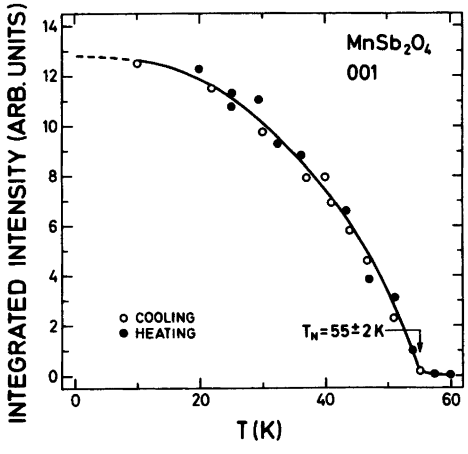

Fig. 4. Integrated intensity of antiferromagnetic 001 reflection *versus* temperature for $MnSb_2O_4$.

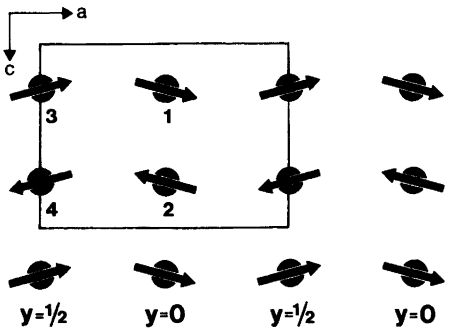

Fig. 5. Magnetic structure of $MnSb_2O_4$ projected along [010]. For convenience the moments, which are undefined within (001), are shown parallel to *a*. Relative heights above projection plane are indicated. For numbering of the Mn atoms see text.

diffraction technique leaves the direction of the moments undetermined within the basal plane. The total moment, $\mu_{tot}=4.52(13)\ \mu_B$, is somewhat smaller than the 2*S* value derived from the magnetic susceptibility data. The resulting magnetic structure is depicted in Fig. 5.

A comparison of the present magnetic structure data with those reported in Refs. 7, 8 is pertinent, but this task is hampered by apparent inconsistencies in the latter papers. However, an important point to note is that Gavarri and Hewat[8] emphasize that the co-operative magnetic properties of $MnSb_2O_4$ strongly depend on the degree of crystallization and imperfections (*e.g.* the unreacted residue) of the samples. The present value of $T_N=55\pm2$ K agrees well with $T_N=60\pm5$ K reported in Ref. 8, whereas there would be a substantial discrepancy with Ref. 7 if the statement "cancellation of the magnetic moment observed at 95 K" is to be interpreted literally. The three studies concur that the major contribution originates from an *A* mode, but the details of the magnetic structure differ. According to Ref. 7 the magnetic moment (pure A_x mode) is 3.8 μ_B at 6 K. (An error estimate is not given in Ref. 7, but $\mu_x=\mu_{tot}=3.8\pm0.8\ \mu_B$ is quoted in Ref. 8.) Ref. 8 specifies the components of the magnetic moment (A_x,A_y,A_z modes) as 3.5, −3.5, 0.2 μ_B at 4.5 K which is inconsistent with $\mu_{tot}=5.1\pm0.3\ \mu_B$ given for the same temperature in the same paper. These results differ from the present findings with respect to the overall magnitude as well as the arrangement of the moments. The present $\mu_{tot}=4.5\pm0.3\ \mu_B$ (error limit taken as twice the *calculated* standard deviation) falls between the earlier values, and taking the error limits into account it may just about be consistent with both of them. The arrangements of the moments reported in Refs. 7,8 are not compatible with the present findings. A misprint of 0.2 for 1.2 μ_B in the *z* component of the magnetic moment would remove the mentioned internal inconsistency of Ref. 8, and this would also *reduce* the discrepancy with the present findings.

Utilization of the temperature dependence of the integrated intensity of 001 (Fig. 4) to extract μ_0 and β of the expression $\mu=\mu_0\ (1-T/T_N)^\beta$ gives $\mu_0=4.3$ and $\beta=0.36$ as compared with 5.3 and 0.50, respectively, reported by Gavarri and Hewat.[8] Much weight should perhaps not be given to the difference in β, but the distinction in μ_0 lends support to the conclusion that the present value for the magnetic moment of $MnSb_2O_4$ is significantly lower than found by Gavarri and Hewat.[8]

The magnetic moments of $MnSb_2O_4$ are mainly confined to the *ab* plane and antiferromagnetically arranged within the *T*−*T* chains. According to Gavarri and Hewat[8] the magnetic moments of $NiSb_2O_4$ order ferromagnetically and mainly parallel to the *c* axis. These findings concur with the exchange interaction models of Goodenough[19] and Motida and Miyahara.[20] The estimated value $\theta=-210$ K by the latter authors for $MnSb_2O_4$ agrees well with the observed value of -190 ± 20 K.

REFERENCES

1. Tamman, G. *Z. Anorg. Allg. Chem. 149* (1925) 78.
2. Ståhl, S. *Ark. Kemi Mineral. Geol. B 17* (1943) 1.
3. Wanmaker, W.L., Hoekstra, A.H. and Verriet, J.G. *Recl. Trav. Chim. Pays–Bas 86* (1967) 537.
4. Gonzalo, J.A., Cox, D.E. and Shirane, G. *Phys. Rev. 147* (1966) 415.
5. Gavarri, J.R., Vigouroux, J.P., Calvarin, G. and Hewat, A.W. *J. Solid State Chem. 36* (1981) 81.
6. Gavarri, J.R. *J. Solid State Chem. 43* (1982) 12.
7. Gavarri, J.R., Calvarin, G. and Chardon, B. *J. Solid State Chem. 47* (1983) 132.
8. Gavarri, J.R. and Hewat, A.W. *J. Solid State Chem. 49* (1983) 14.
9. Deslatters, R.D. and Henins, A. *Phys. Rev. Lett. 31* (1973) 972.
10. Hewat, A.W. *The Rietveld Computer Program for the Profile Refinement of Neutron Diffraction Powder Patterns Modified for Anisotropic Thermal Vibrations,* UKAERE Harwell Report RRL73/897 (1973).
11. Rietveld, H.M. *J. Appl. Crystallogr. 2* (1969) 65.
12. Koester, L. and Yelon, W.B. In Yelon, W.B., Ed., *Neutron Diffraction Newsletter,* Missouri 1983.
13. Watson, R.E. and Freeman, A.J. *Acta Crystallogr. 14* (1961) 27.
14. Roth, W.L. *Phys. Rev. 110* (1958) 1333.
15. Feyek, M.K. and Leciejewicz, J. *Z. Anorg. Allg. Chem. 336* (1965) 104.
16. Svensson, C. *Acta Crystallogr. B 30* (1974) 458.
17. Svensson, C. *Acta Crystallogr. B 31* (1975) 2016.
18. Bertaut, E.F. *Acta Crystallogr. A 24* (1968) 217.
19. Goodenough, J.B. *Phys. Rev. 117* (1960) 1442.
20. Motida, K. and Miyahara, S. *J. Phys. Soc. Jpn. 28* (1970) 1188.

Received December 10, 1984.